

Investigation of the Gravity Anomalies within Brass and Environs, Niger Delta Area, Nigeria: Implications for Hydrocarbon Prospectivity

¹Egwuonwu, Gabriel Ndubuisi*, ²Ibe, Stephen Onyejiuwaka, ¹Ejike, Kingsley Nnaemeka, ³Orji, Obinwa, and ⁴Ombu, Righteous Emmanuel

¹Department of Physics and Industrial Physics, Nnamdi Azikiwe University, Awka, Anambra State, Nigeria

²Department of Physics, Federal University Otuoke, Bayelsa State, Nigeria.

³Department of Physics, Clifford University, Owerri, Nigeria.

⁴Department of Physics with Electronics, Federal Polytechnic Ekowe, Bayelsa State.

*Corresponding Author's

DOI: <https://doi.org/10.51584/IJRIAS.2023.8606>

Received: 24 May 2023; Accepted: 01 June 2023; Published: 03 July 2023

Abstract: The airborne gravity data over Brass Area and environs, Niger Delta Area, Nigeria were processed and interpreted in order to delineate the sedimentary thickness within the basin and map out places with the potentials for hydrocarbon formation, accumulation and migration. The geological structures, depths and structural trends within the area were investigated using Total Horizontal Gradient, Tilt Derivative, Analytical Signal Filters and Euler Deconvolution techniques. The results from Euler depths showed that the sedimentary thickness and structural depths within the area range from about 1.6 to over 17.4 km. The area predominantly has NE-SW structural trend with minor NW-SE trend. The sediment thickness and structural endowment of the area prompted the classification of Egeregere, Brass, Spiff Town, Kirikakiri Areas in the northern and the southern parts of the area as zones of very viable potentials for hydrocarbon generation, accumulation and migration.

Keywords: Brass Area, Sedimentary Thickness, Structural Complexity, Structural Faults, Intrusive Activities, Hydrocarbon potential.

INTRODUCTION

Geoscientists have described gravity method as the foundation of Geophysics (Osazuwa, 2006; Ibe and Anekwe, 2016). Density is an important parameter for the determination of gravity anomalies. The accuracy of Bouguer anomalies and their interpretation depend greatly on the assumed density of rocks or more accurately the density differences of rocks. It is known that gravity anomalies result from the differences in densities, or density contrasts between rock bodies and their surroundings (Egwuonwu *et al.*, 2021). Gravity generally relates to other geophysics disciplines, directly or indirectly. For example, both magnetics and gravity are potential fields, derivable from the inverse square law and there is an empirical relationship between them popularly known as the Poisson relation. This relation makes it possible to determine the pseudo field of one from the measured field of the other. In oil and gas Industry seismic remains the primary method for exploring hydrocarbon prospects. However, it is rational to implement inexpensive geophysical exploration methods before seismic detailing (Telford *et al.*, 1990). The use of magnetic and/or gravity techniques for basin delineation at a regional scale, especially in hydrocarbon exploration, is well-known (Osazuwa, 2006; Ibe and Anekwe, 2016). Hydrocarbon exploration applies gravity method in detecting faults and igneous intrusions, forming structural traps for hydrocarbon. Magnetics is commonly used with gravity as low-cost methods for mapping out structures and delineating the sediment thickness during the beginning phases of exploration. Evaluation of structural systems aims to target structural traps and sediment thickness to assess the maturity of the sediments within the target basin.

In November 2020, Bayelsa State hosted the National Council on Hydrocarbon Summit, where the government revealed its interest in identifying new petroleum prospects in the state. The growing interest in new hydrocarbon prospects by the government is what instigated this research. One of the fundamental features that affect the formation of hydrocarbon in a basin is the thickness of the sediment (Wright *et al.*, 1985; Anyanwu and Mamah 2013; Ibe and Uche 2021). Another fundamental feature that affects the formation of hydrocarbon in a basin is the structural endowment of the basin (faults and fractures) which could serve as migratory pathway for hydrocarbon or hydrothermal fluid (Uche *et al.*, 2020). There was need to delineate the thickness of the sediments and structural endowment of Brass Area and environs with high resolution geophysical data. This study used high resolution airborne gravity data to appraise the hydrocarbon potential of the study area. The research focused on the application of gravity method in delineation of structures and sediment thickness underlying Brass Area and environs; hence, highlighting the basin's structural and sedimentary endowments favourable for hydrocarbon generation, accumulation and migration. The geologic features that enhanced the generation and accumulation of oil within the area were highlighted in this

study. This research therefore identified new suitable prospect areas for localized studies. Hence, the results of this study will be very useful for 2D seismic survey planning for identifying new petroleum prospects in the study area. The results will serve as a guide in ensuring suitable angles of the lines to the structures and focusing on the most interesting parts of the basin with potential for hydrocarbon accumulation.

Geology and Location of the Study Area

The study area is bounded by longitudes 6°00'00"E and 6°30'00"E and latitudes 4°00'00" and 4°30'00"N; it covers a surface area of about 3,025 km². It shares boundary with Sangakubu in the north, Kambora in the northwest, Sengana in the southwest, Botokiri in the east and Atlantic Ocean in the south. It falls within the humid tropical region with two distinct seasons, the rainy season, from March to October, and dry season, from November to March. The study area is located in Bayelsa State, Nigeria (Figure 1) and is predominantly Ijaw, with the Ijaw languages being widely spoken. Being in the Niger Delta Region, the study area has a riverine and estuarine setting, with bodies of water within the place preventing the development of significant road infrastructure. Many communities within the place are almost completely surrounded by water, making them inaccessible by road. The inhabitants of the communities are mainly fishermen and farmers.

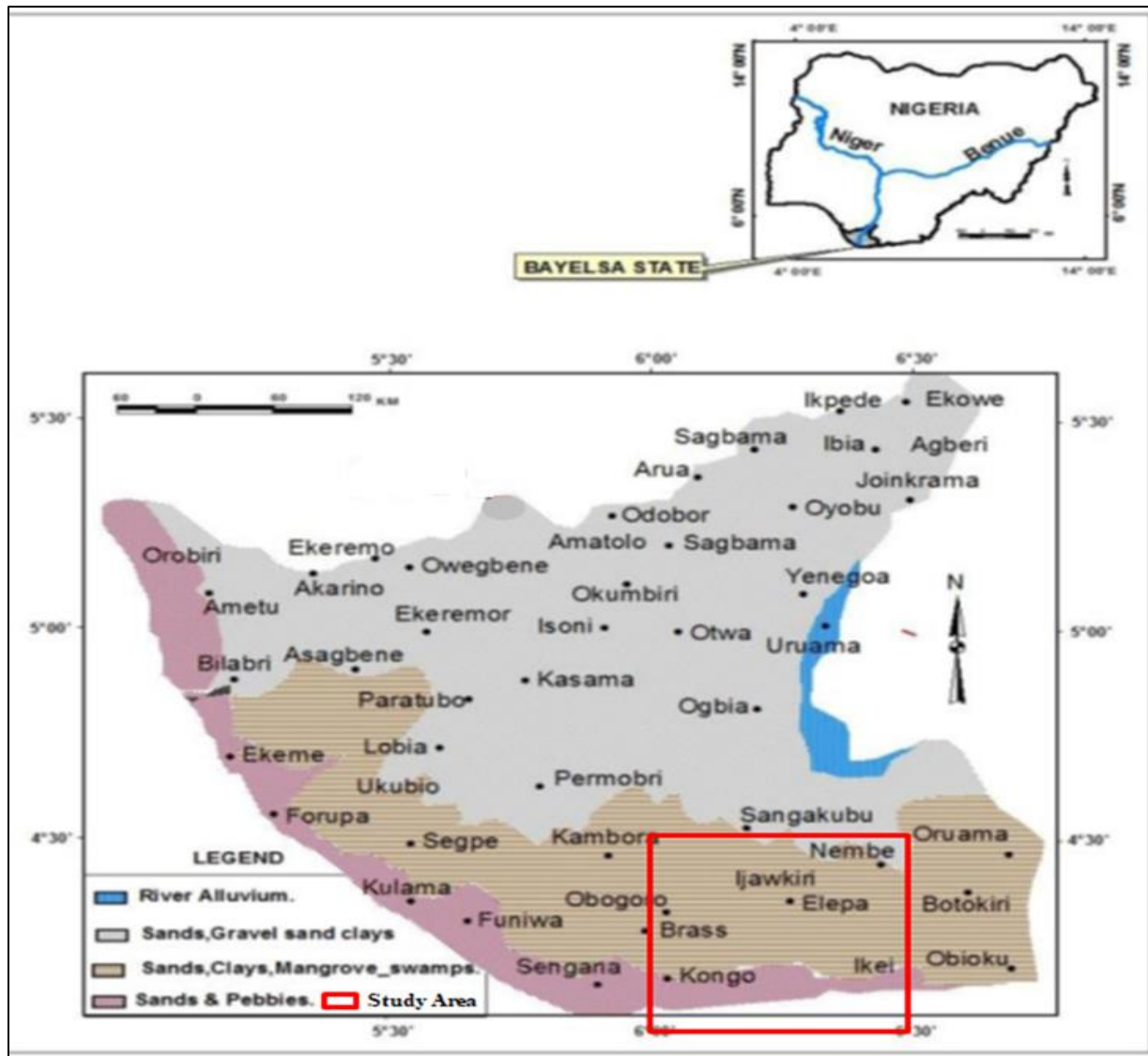


Figure 1: Geology Map of the Study Area.

II. Methodology

Data acquisition

The gravity data used for this study were acquired by Fugro Airborne Survey and the Nigerian Geological Survey Agency. The data were acquired along NW– SE flight lines at 500 m line spacing and 80 m terrain clearance. The study area consists of one square block of airborne gravity Map Sheet (334- Brass) which covers an area of about 3,025km². The acquired gravity data were processed, and the data grid was developed by employing a minimum curvature algorithm at 100 m grid cell size.

Data Enhancement and Interpretation Techniques

Regional - Residual Separation

Separation of regional and residual anomaly fields was done using Trend analysis in which a linear trend surface was fitted into the Bouguer gravity field data by a multiple regression technique for the purpose of removing the regional gravity field. The linear surface fitted was removed from the regional component to obtain the residual (gravity) anomaly map that was interpreted.

$$freeairgravity = Regionalfield + Residualfield \quad 1$$

$$Residualfield = freeairgravity - fittedSurface/Regional \quad 2$$

The Regional Field can be represented using the trend surface equation expressed as the regional field:

$$RegionalField = a + bx_i + cy_j \quad 3$$

Where, a, b and c are constants, x_i and y_j are coordinates in x and y directions.

Let Z_{ij} = the observed Bouguer Field at ij^{th} data point.

Therefore,

$$freeairgravity(Z_{ij}) = (a + bx_i + cy_j) + ResidualField \quad 4$$

Hence,

$$ResidualField = Z_{ij} - (a + bx_i + cy_j) \quad 5$$

Analytic signal

Analytical signal is a popular gradient enhancement, which is related to gravity fields by the derivatives. Roest *et al.*, (1992), showed that the amplitude of the analytic signal can be derived from the three orthogonal gradients of the total gravity field using the expression:

$$|A(x, y)| = \sqrt{\left(\left(\frac{dm}{dx}\right)^2 + \left(\frac{dm}{dy}\right)^2 + \left(\frac{dm}{dz}\right)^2\right)} \quad 6$$

Where $A(x, y)$ is the amplitude of the analytical signal at (x, y) and m is the observed gravity anomaly at (x, y) . By examining its profile across a gravity source, the analytic signal was used in the interpretation to provide an indication of the edges of the causative body. The maximum value of the analytic signal determines the edges of the gravity body.

Tilt Angle Derivative

Since the amplitude of gravity signature depends on gravity field strength and to some extent the depth of gravity sources, lower amplitude signature may be suppressed at the expense of higher amplitudes. For this reason, the edge-detection filters are normally applied for delineating linear features without necessarily diminishing the long-wavelength anomalies (Oruc and Selim, 2011). The Tilt derivative filter, TDR (a very good edge detection filter) brings out short wavelength and reveals the presence of gravity lineaments. Verduzco *et al.* (2004) showed that tilt derivative filter also performs an automatic-gain-control (AGC) filter which tends to equalize the response from both weak and strong anomalies. Hence, the filter provides an effective way to trace out along striking anomalies. The tilt angle is defined as

$$T = \tan^{-1} \left(\frac{\frac{df}{dz}}{\sqrt{\left(\frac{df}{dx}\right)^2 + \left(\frac{df}{dy}\right)^2}} \right) \quad 7$$

Horizontal Gradient

This Calculates the n^{th} horizontal derivatives in the x and y directions. This process involves a phase transformation as well as an enhancement of high frequencies. Horizontal gradient method is least susceptible to noise in the data. The phase transformation generally has the result of producing anomaly peaks approximately located over the edges of wide bodies and the enhancement of the high frequencies sharpens these peaks to increase the definition of the body edges. This quality of horizontal derivatives is used to map body outlines (Milligan and Gunn, 1997). Horizontal gradient is given as,

$$\text{Horizontal gradient } (HG_{x,y}) = \left[\left(\frac{\partial g}{\partial x}\right)^2 + \left(\frac{\partial g}{\partial y}\right)^2 \right]^{1/2} \quad 8$$

where $\frac{\partial g}{\partial x}$ and $\frac{\partial g}{\partial y}$ are the horizontal gradients of the gravity field in the x and y directions, respectively.

Euler Depth

A technique known as Euler deconvolution was developed to process gravity data and to convolve them to a point source at depth. For an arbitrary specific structural index the depths and locations for various targets can be resolved from the following first order derivatives (x,y and z).

$$(x - x_0) \frac{dT}{dx} + (y - y_0) \frac{dT}{dy} + (z - z_0) \frac{dT}{dz} = N(B - T) \quad 9$$

Where (x_0, y_0, z_0) is the source of gravity anomaly, (x, y, z) is the total gravity field detection points, B is the regional gravity field N is the fall-off rate gravity field measurement also known as the structural index (SI).

III. Results and Discussion

Qualitative Interpretation of the Gravity data

The Bouguer anomaly map (Figure 2) revealed the density distribution within the study area. The colour distribution is indicative of both shallow and deep gravity anomalies. The study area is generally characterized by long wavelength anomalies; these are indicative of deep-seated bodies. This raster colour map shows three types of anomalies within the study area. High anomalous zones (magenta to red colour) are associated with high density structures. Moderate anomalous zones (yellow to green) are associated with moderate density structures, while low anomalous zones (blue colour) are associated with low density structures. The high Bouguer gravity anomaly amplitudes range from 38.63 mGal to 68.18 mGal, the moderate Bouguer gravity anomaly amplitudes range from 23.14 mGal to <38.63 mGal, while the low Bouguer gravity anomaly amplitudes range from 7.48 mGal to <23.14 mGal. The study area is predominantly underlain by NW-SE structures with the offshore area (southern part) characterized by high density bodies displaying high Bouguer anomalies and the onshore area (northern part) characterized by both moderate and low density bodies displaying moderate and low Bouguer anomalies. Beletiam, Clarendon Island, Egeregere, Akassa, Funumu and Egwema Pogu Areas are characterized by NE-SW trending high Bouguer anomalies; Brass, Spiffs Town, Dikimatubu and Kirikakiri Areas are characterized by an almost NNW-SSE trending anomalies. The NW-SE predominant trends in the study area are interpreted to have controlled the strike of the sediments within the area while the localized NE-SW and NNW-SSE trends is controlled folding and faulting of sediments in the area.

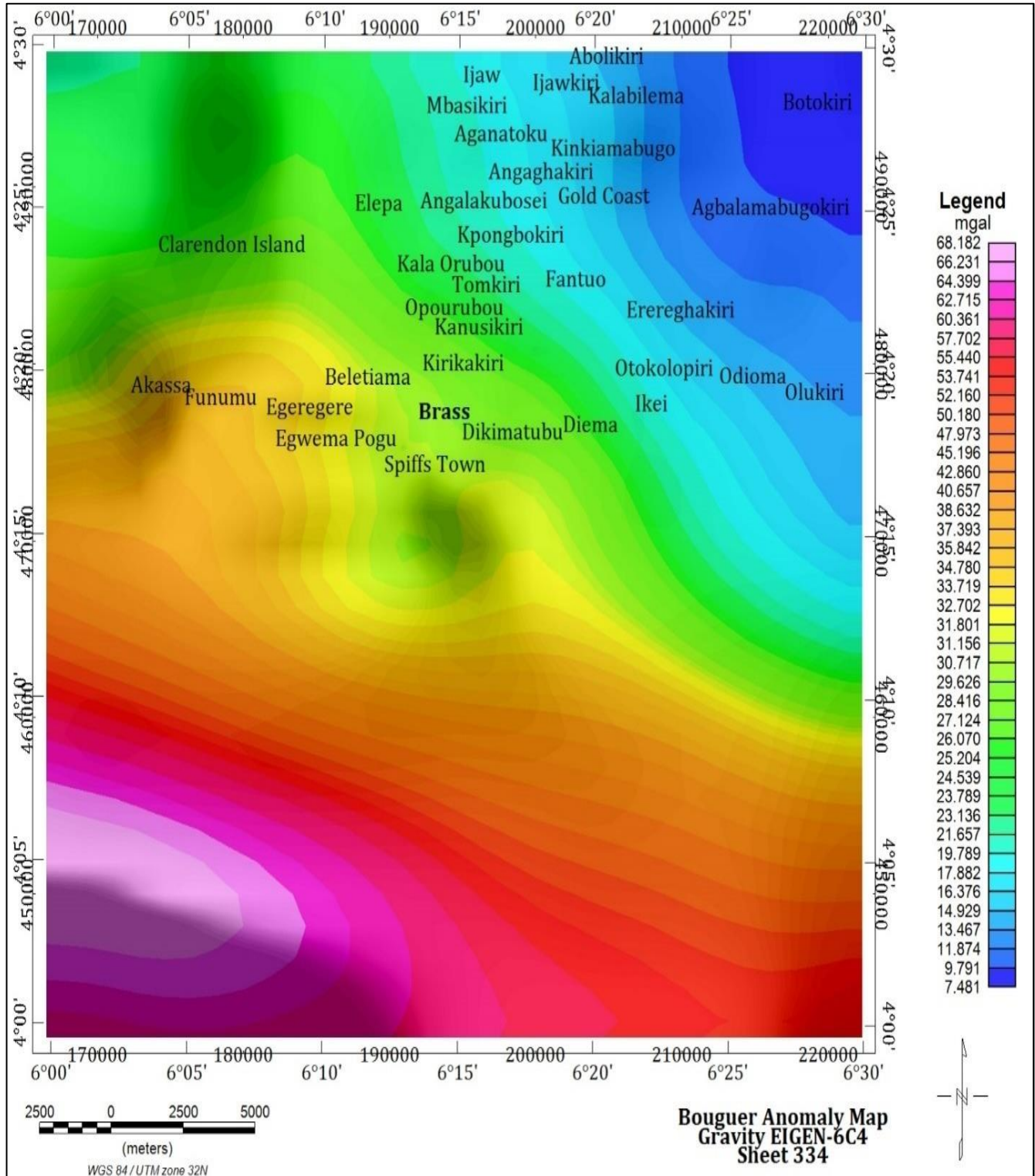


Figure 2: Bouguer Anomaly Map of the Study Area

The regional gravity map of the study area (Figure 3) has a NW-SE gradient trend with high amplitude at the southwestern part of the area and low amplitude at the northeastern part of the area. This gradient trend is most likely due to the thickening of sediments in the southwestern part of the study area (offshore) and thinning of sediments in the northeastern direction (onshore). The regional anomaly is characterized by large positive anomalies ranging from 6.89 mGal to 68.68 mGal.

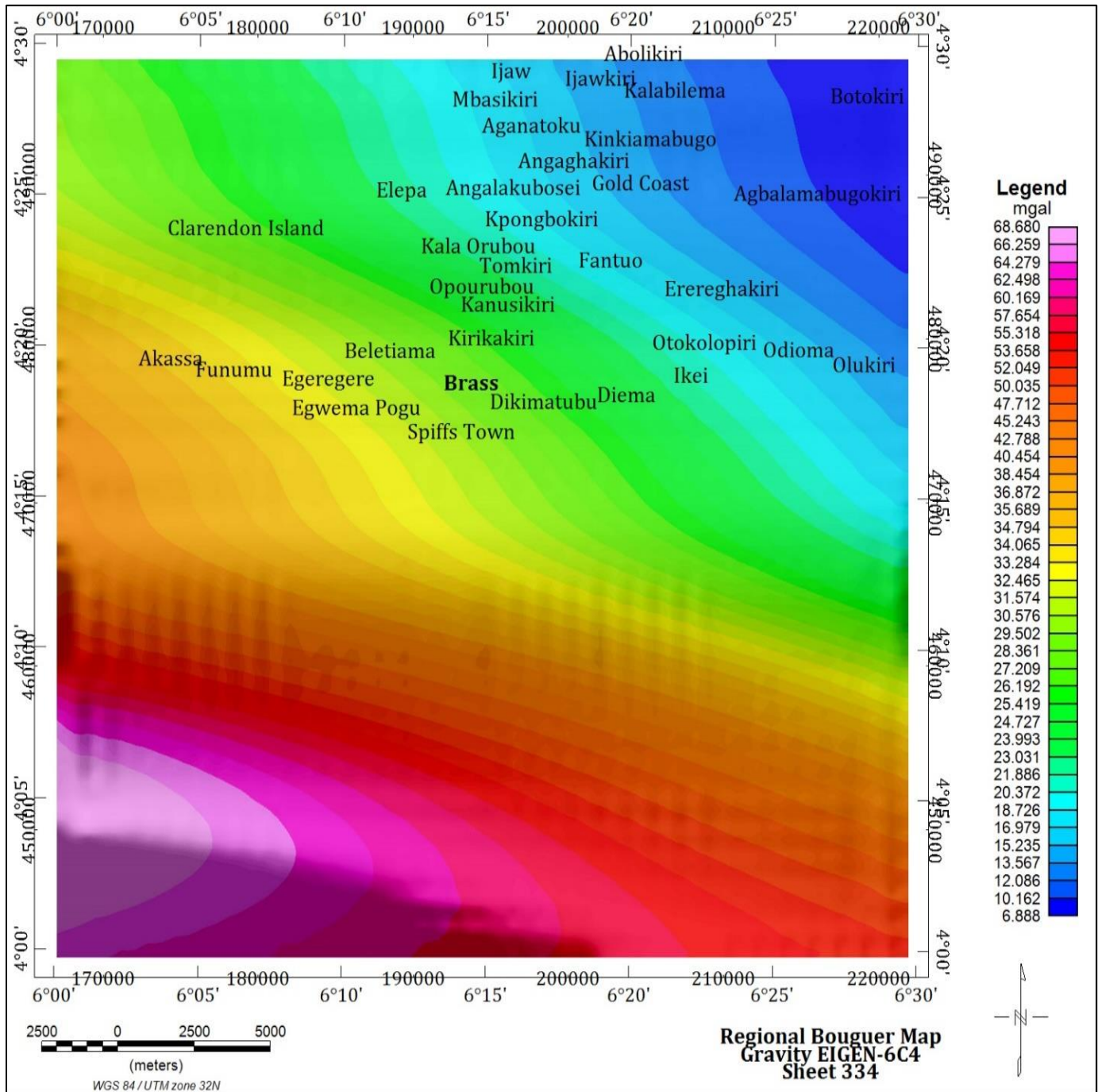


Figure 3:Regional Gravity Field Map of the Study Area

The computed residual anomaly map of the study area (Figure 4) shows anomaly values ranging from -7.7 mGal to 4.4 mGal. Brass, Kirikakiri, Dikimatubu, Diema and Spiffs Town Areas are characterized by high density anomalies with NW-SE trend and gravity range of 2.2 mGal to 4.4 mGal. Elepa, Clarendon Island, Funumu, Egeregere and Egwema Pogu Areas are also characterized by high anomaly range of 2.2 mGal to 4.4 mGal with the high anomalous zone having NNE-SSW trend. Ijaw, Aganatoku, Analakubesei, Kala Orubou and Tomkiri Areas have anomaly range of 1.1 mGal to <2.4 mGal. The northeastern part of the study area, within Botokiri, Agbalamabugokiri, Erereghakiri, Ikei, Odioma and Olukiri Areas are characterized by low gravity anomaly ranging from -0.2 mGal to -7.7 mGal. The offshore areas (southern part of the study area) are characterized by anomaly range of -7.7 mGal to 2.6 mGal. The high anomaly values observed within the southwestern part of the study area have a NW-SE trend and are interpreted to occur within the continental slope.

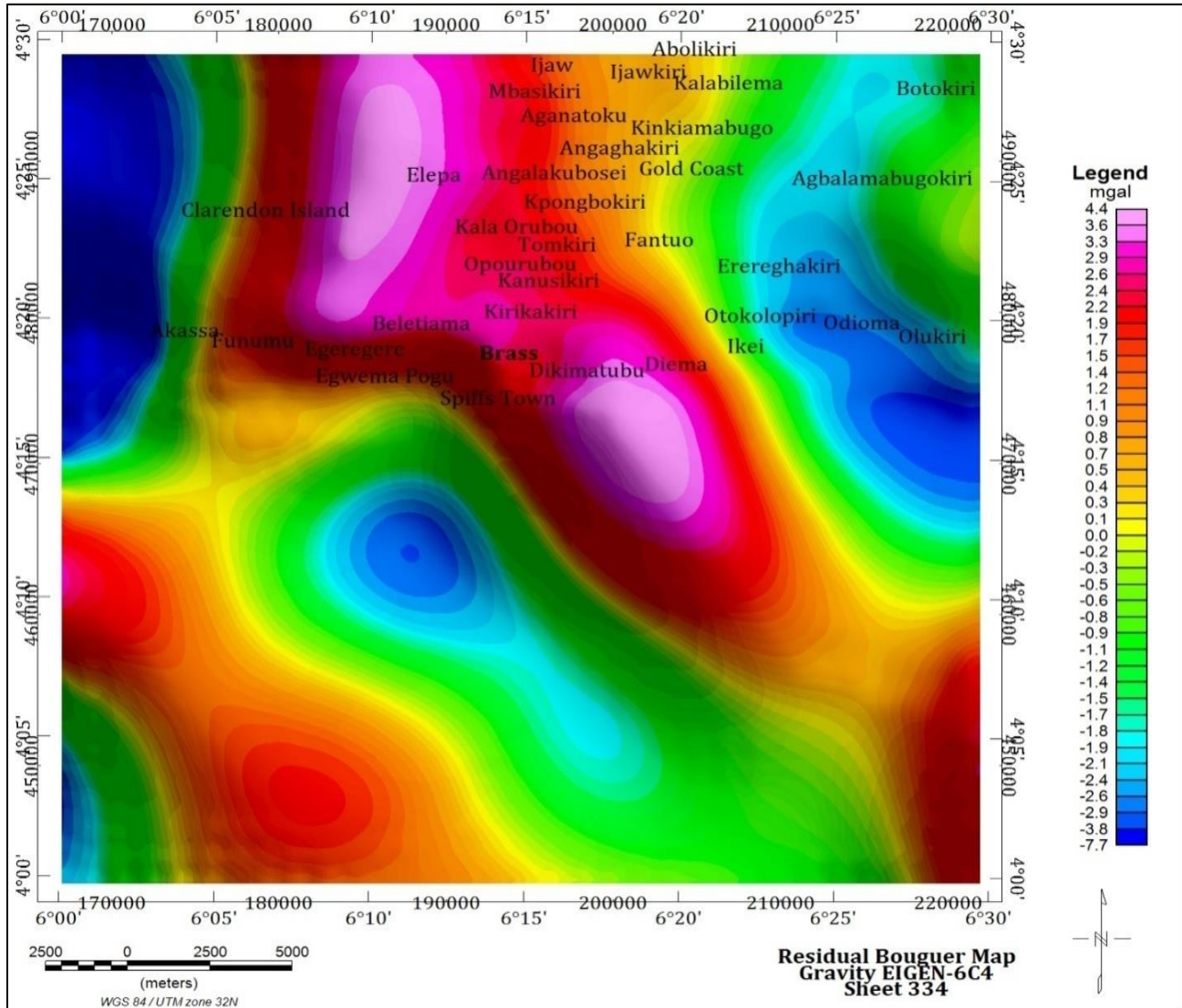


Figure 4: Residual Gravity Anomalies Map of the Study Area

Structural Interpretation of the Derivative Maps

To enhance the gravity structures of the study area, horizontal gradients, tilt derivative and analytical signal filters were applied to the computed Bouguer gravity anomaly data. The application of these edge enhancement techniques over the residual gravity anomalies delineated the subsurface features corresponding to different depths. The lineaments were mapped by using targeting the peak and trough of gravity anomalies from total horizontal derivative, tilt derivative and analytic signal anomaly maps which are based on different anomaly patterns.

The total horizontal derivative map (Figure 5) delineated edges from shallow structures, depicting that Brass, Spiffs Town, Dikimatubu, Egwema Pogu, Egeregere and Beletiamo Areas are characterized by high anomaly gradients ($3.9 \times 10^{-4} \text{ mGal/m}$ to $5 \times 10^{-4} \text{ mGal/m}$) that have both NE-SW and NW-SE trends. Kala Orubou and Opourubou Areas are characterized by high anomalous gravity gradients ($3.9 \times 10^{-4} \text{ mGal/m}$ to $1.08 \times 10^{-3} \text{ mGal/m}$) with NNE-SSW trend. A long stretching high gravity gradient ($2.9 \times 10^{-4} \text{ mGal/m}$ to $3.9 \times 10^{-4} \text{ mGal/m}$) extends from Kirikakiri town, through Tomkiri, Angalakubosei and Mbasikiri Areas to Ijaw Area. Abolikiri, Kalabilema and Gold Coast Areas are characterized by a broad high gravity gradient anomaly ($3.2 \times 10^{-4} \text{ mGal/m}$ to $4.4 \times 10^{-4} \text{ mGal/m}$) that has NE-SW trend. Otokolopiri, Ikei and Diema Areas are characterized by high gravity gradient ($2.9 \times 10^{-4} \text{ mGal/m}$ to $3.9 \times 10^{-4} \text{ mGal/m}$) that has NW-SE trend. At the northeastern part of the study area, Agbalamabugokiri Area is characterized by a NW-SE trending high gravity gradient, while Botokiri and Olukiri Areas are characterized by high gravity gradient with NE-SW trend.

South and southwestern parts of Akassa and Funumu Areas (offshore) are characterized by numerous high gravity gradient ($3.9 \times 10^{-4} \text{ mGal/m}$ to $1.08 \times 10^{-3} \text{ mGal/m}$) structures with both NW-SE and NE-SW trends. The offshore structures are characterized by gravity gradients with both low and high amplitudes. The high gravity gradient anomalies predominantly have NW-SE trend with minor NE-SW trend. The low gravity gradient anomalies predominantly have NE-SW structural trend with minor NW-SE trend.

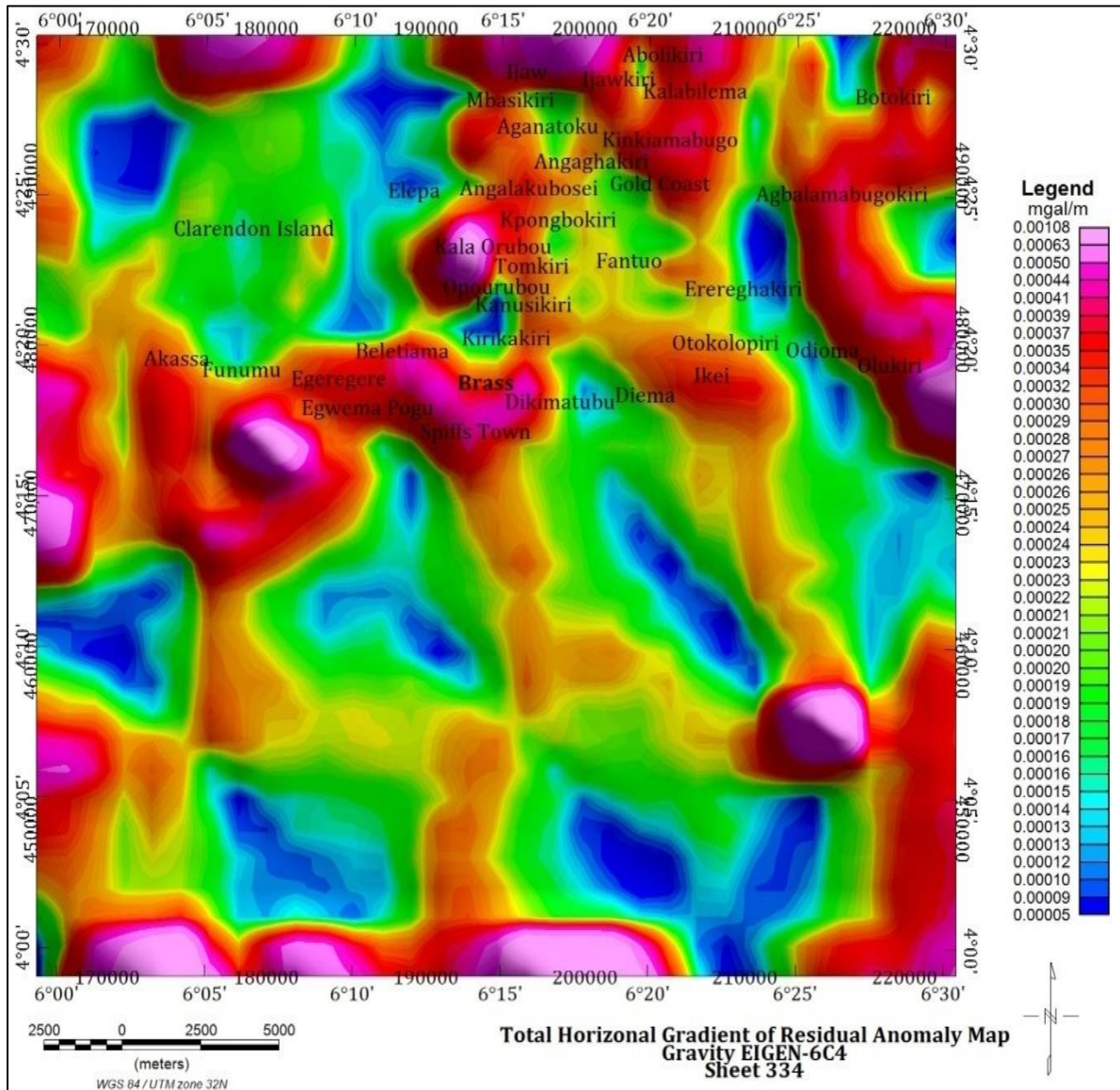


Figure 5: Total Horizontal Derivative Map of the Study Area

The analytic signal map (Figure 6) delineated edges from shallow and medium depth structures showing only three major high gravity gradient anomalies. The first high gravity gradient anomalies extend from the southeastern part of Spiffs Town, through Diema Area to Ikei and Otokolopiri communities and have NE-SW trend. The second high gravity gradient anomalies with NW-SWE and NNE-SSW trends extend from Egeregere and Funumu Areas through Clarendon Island to the west of Ijaw. The third high gravity gradient anomalies delineated within Brass, Spiffs Town and Egwema Pogu Areas have NW-SW trend.

The analytic signal delineated low gravity gradient anomalies within the onshore area which have major NW-SE and minor NE-SW trends. The offshore areas are generally characterized by moderate to low gravity gradients of analytic signal, except at the western and eastern parts of the study area which show presence of high density structures. Figure 6 also shows that the low density structures within the offshore area predominantly have NE-SW trend, while the high density structures within the area have NNW-SSE trend.

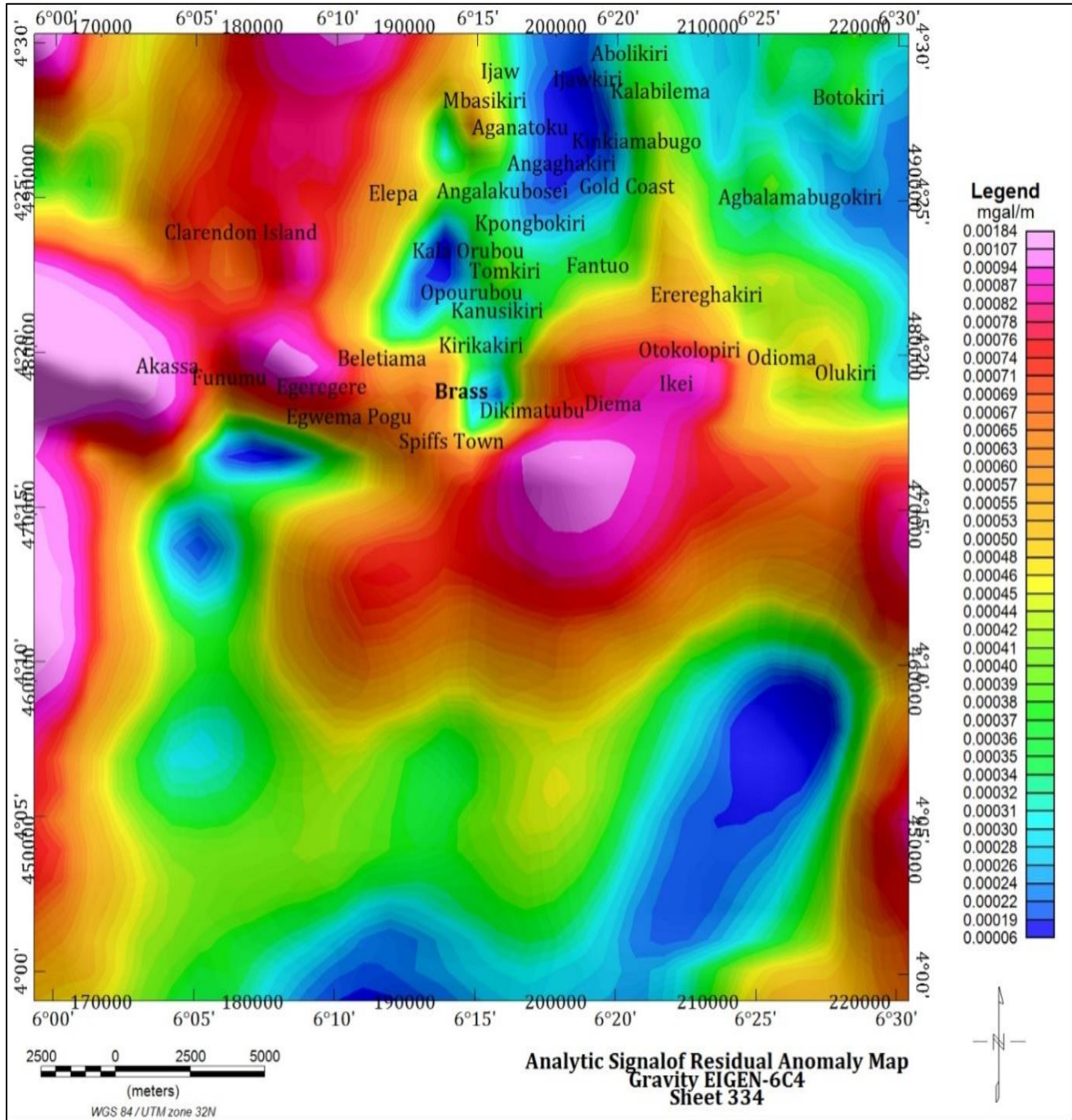


Figure 6: Analytic Signal map of the study area

The tilt derivative map (Figure 7) delineated all the structural edges inclusive of the shallow and medium depth sources. The tilt derivative map reflected the gravity anomaly distribution across Brass Area and its boundary communities. It highlighted the density anomalies effects close to the surface at the expense of deep sited bodies. Its analysis shows that it enhances the edges of anomalies and improves the superficial features. The analysis also shows high gravity gradients within Brass, Diema, Spiffs Town, Kirikakiri, Opourubou, Orubou, Elepa, Clarendon Island and Egeregere Areas. The Gold Coast, Angaghakiri, Ijaw, Mbasikiri, Angalakubosei, Akassa and Funuma Areas are characterized by moderate gravity gradients while Botokiri, Agbalamabugokiri, Erereghakiri, Otokolopiri, Odioma and Olukiri Areas characterized by low gravity gradients. The offshore area within the study area is characterized by negative Bouguer gravity gradients except at the southwestern part of the study area where there is a large NW-SE trending high gravity gradient.

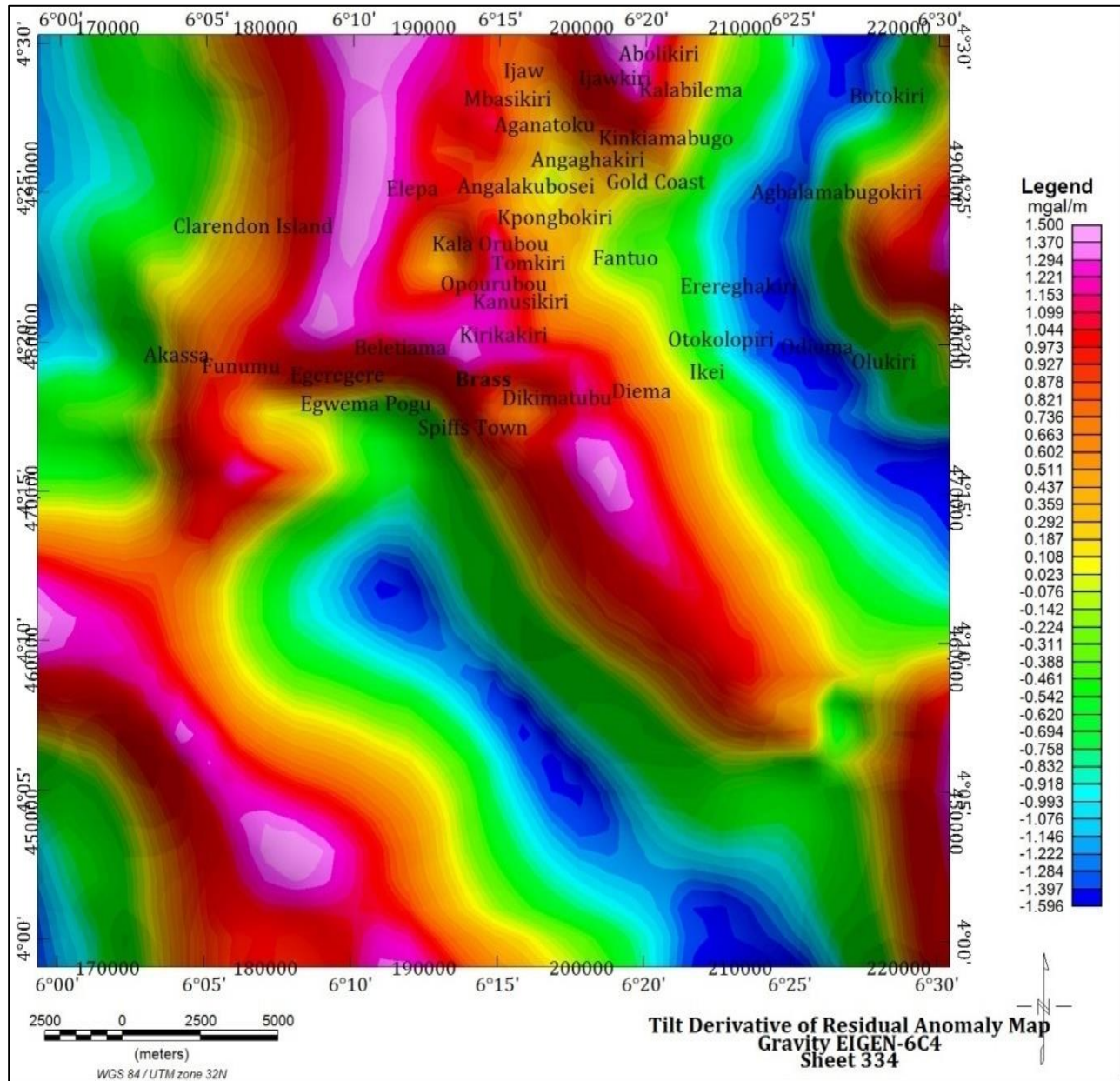


Figure 7: Tilt derivative map of the study area

Euler depth Map

The Euler depth solutions map (Figure 8) reflects the depth to geological structures/bodies responsible for the Bouguer gravity anomalies in the study area. The shallowest geological structures are represented by the red to pink colour Euler depths. Moderate Euler depths are represented by green colour, while the deepest structures are represented by blue colour Euler depths. Geological structures within Angaghakiri, Angalakubosi, Kpongbokiri and Kala Orubou Areas have depths ranging from 2.0 km to 3.4 km. Structures within Clarendon Island, Akassa and Funumu Areas have depths ranging from 1.6 km to 5.8 km. The geological structures within Brass Area have depths between 4.5 km and 9.9 km while the structures within Beletiam, Egeregere, Pogu and Spiffs Town Areas have a depth range of 4.7 km to over 17.4 km with the deepest structure located at Spiffs Town. Fantur, Diema, Otokolopiri and Ikei Areas have geological structures located at a depth range of 3.6 km to 6.6 km while the structures within Odioma and Olukiri Areas are located at depths ranging from 4.7 km to 5.5 km. The deepest structures within the offshore area are located at the southeastern part of the study area with depths ranging from 4.8 km to 17.4 km. These computed depths are in agreement with the works of Lucas and Omodolor (2018), Lucas and Odedede (2012) and Murat, (1972) which stated that the delta complex contains a sedimentary thickness of over 12,000 m, which consists of three Anachronous Lithostratigraphic Units.

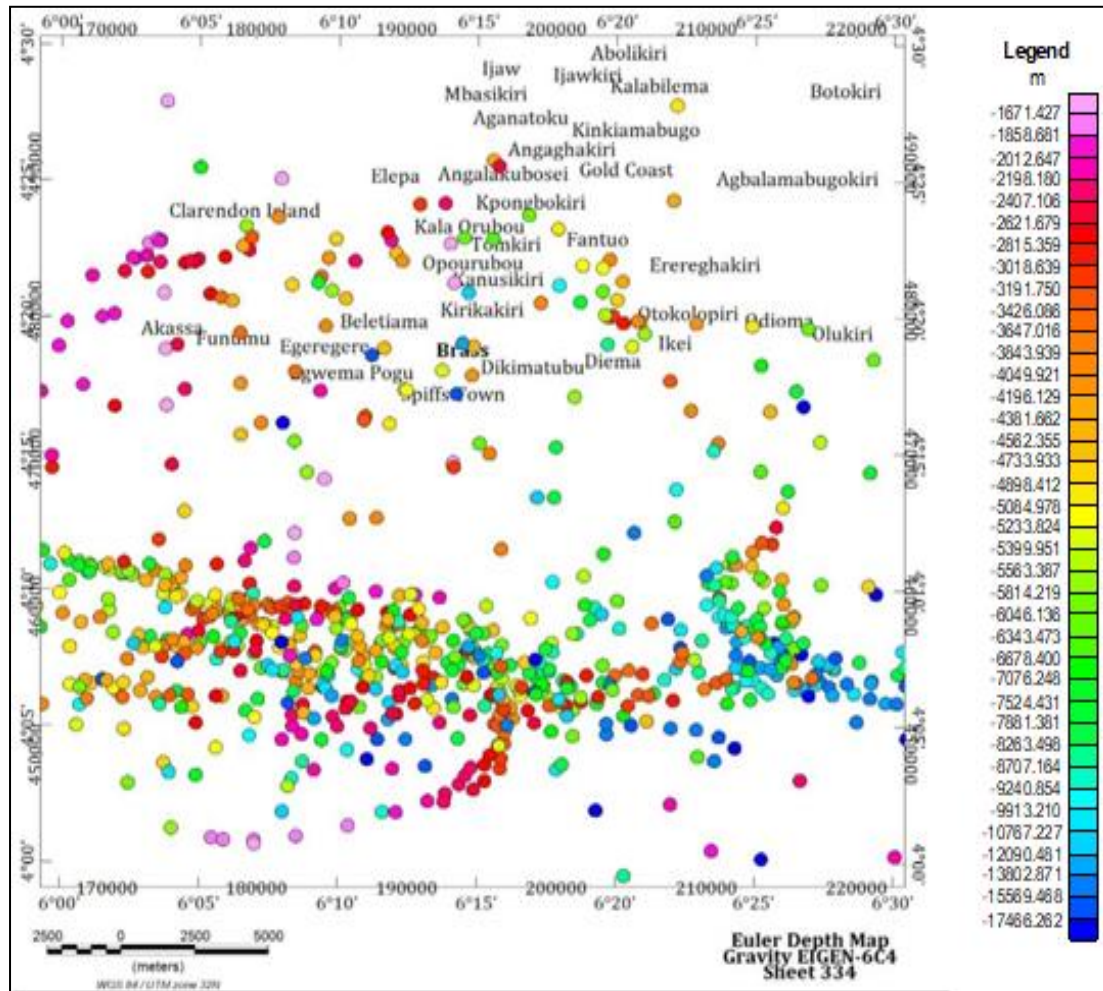


Figure 8. Euler depth map, point distribution is an indication of the anomaly sources depth

The interpretation of the residual field map (Figure 4), the derivative maps (Figures 5-7) and the Euler depth map (Figure 8) suggests that the study area is structurally controlled sedimentary basin with lineaments and both regional and minor faults associated with fracture systems and intrusive activities. The fracture systems developed due to stress imposed on the crust. Fracture gaps representing discontinuities are favourable areas for hydrocarbon accumulation. Such fracture systems delineated within the entire study area are predominant in the southern part (offshore area). These also suggest structural complexity and deformation of the basin.

The Euler depth map suggests that the depths to these structures within the study area range from about 1.6 to >17.4 m with deepest structures predominantly located in the southern parts of the area. Wright *et al.* (1985) and Ibe and Uche (2021) had observed that one of the fundamental features that affect the formation of hydrocarbon in a basin is the thickness of the sediment. It is known that the minimum thickness of sediment required to achieve the threshold temperature of 115°C for the commencement of oil formation from organic remains is 2.3 km when all other conditions for hydrocarbon accumulation are favourable and the average temperature gradient of 1°C for 30 m obtainable in oil rich Niger Delta is applicable (Wright *et al.*, 1985). These further suggest that most places within the study area have both the sediment thickness and structural complexity favourable for hydrocarbon generation and accumulation and the southern part of the study area is more deformed than other places in the area.

IV. Conclusion

This study shows that the depths to the structures within the study area range from about 1.6 to >17.4 m with deepest structures predominantly located in the southern parts of the area. The area is structurally controlled sedimentary basin with both regional

and minor faults associated with fracture systems and intrusive activities. The fracture gaps representing discontinuities are favourable areas for hydrocarbon accumulation. The area predominantly has NE-SW structural trend with minor NW-SE trend. Most places within the study area have both the sediment thickness and structural complexity favourable for hydrocarbon generation and accumulation and the southern part of the study area is more deformed than other places in the area. The sediment thickness and structural endowment of the study area prompted the classification of some locations within it as zones of very viable potentials for hydrocarbon generation, accumulation and migration. Hence, localized geophysical studies are recommended to be conducted in Egeregere, Brass, Spiff Town and Kirikakiri Areas in the northern part and the southern part of the area which were delineated as hydrocarbon prospect zones in Brass Area.

References

1. Wright, J.B., Hastings, D.A., Jones, W.B. and Williams, H.R. (1985). *Geology and mineral resources of West Africa*. George Allen and Unwin, London. <https://doi.org/10.1007/978-94-015-3932-6>.
2. Ibe, S.O. and Uche, I. (2021). Spectral Re-evaluation of Sediment Thickness within Afikpo Basin and Environs, Southeastern Nigeria, using High Resolution Aeromagnetic Dataset. *International Journal of Advanced Geosciences*, vol. 9 (1), pp. 11-18.
3. Cengiz, O., Sener, E and Yagmurlu, F. (2006). A satellite image approach to the study of lineaments circular structures and regional geology in the Golcuk Crater district and its environs (Isparta, SW Turkey); *J. Asian Earth Sci.* 27(2) 155-163.
4. El Gout, R., Khattach, D. and Houari, MR. (2009). Gravity study of the northern flank of Béni Snassen (Eastern North Morocco): structural and hydrogeological implications. *Mohamed Premier University, Oujda. Bull. Ins Sci., Rabat, Earth Sciences Section*, 31, 61-75.
5. Ibe, S.O. and Anekwe, U. L. (2016). Reliability of Density of Rock Generated from Its P-Wave Velocity in Geophysics Interpretations and Geotechnical Studies. *International Organisation of Scientific Research IOSR- Journal of Applied Geology and Geophysics*. www.iosrjournals.org (IOSR-JAGG). e-ISSN: 2321-0990, p-ISSN: 2321-0982, 4(5): 30 - 36.
6. Lucas F.A and Odedede O. (2012). Lithofacies characterization of sedimentary succession from Late Cretaceous-Tertiary age in Benin west-1, Northern Depobelt, Anambra Basin, Nigeria”, *World Journal of Engineering*, Vol. 9 Issue: 6, pp.513-518.
7. Lucas F.A and Omodolor H.E. (2018). Lithofacies Characterization of Sedimentary Succession from Oligocene to Early Miocene Age in X2 Well, Greater Ughelli Depo Belt, Niger Delta, Nigeria. *Journal of Geosciences and Geomatics*. **2018**, 6(2), 77-84. DOI: 10.12691/jgg-6-2-5
8. Milligan, P. R. and Gunn, P. J. (1997). Enhancement and presentation of airborne geophysical data. *AGSO Journal of Australian Geology and Geophysics*, 17(2):64–774.
9. Murat, R. C. (1972). Stratigraphy and paleogeography of the Cretaceous and lower Tertiary in Southern Nigeria. In *Proc. of the Conf. on African Geology held at Ibadan, Nigeria*. pp. 251-266
10. Oruc, B. and Selim, H. (2011). Interpretation of magnetic data in the Sinop area of Mid Black Sea, Turkey, using tilt derivative, Euler deconvolution, and discrete wavelet transform. *Journal of Applied Geophysics*, 74, 194–204.
11. Osazuwa, I.B. (2006). Gravity: The Foundation of Geophysics and Its Usefulness to Mankind. An Inaugural Lecture, 12th July, 2006, Ahmadu Bello University, Zaria.
12. Roest, W.R., Verhoef, J. and Pilkington, M. (1992). Magnetic Interpretation using the 3-D analytical signal. *Geophysics*, 57:116-125.
13. Telford, W., Geldart, L. and Sheriff, R. (1990). *Applied Geophysics* (second edi).
14. Verduzco, B., Fairhead, J., Green, C. and Mackenzie, C. (2004). New insights into magnetic derivatives for structural mapping. *The Leading Edge*, 23, 116-119.
15. Anyanwu G, Mamah L. (2013). Structural Interpretation of Abakaliki-Ugep; Using Airborne Magnetic and Landsat Thematic Mapper (TM) Data. *Journal of Natural Sciences Research*, Vol. 3, pp. 137-148.
16. Uche I, Ibe SO, Nwokeabia CN. (2020). Curie Depth and Heat Flow Analysis of Ikot Ekpene and Environs, Eastern Niger Delta Basin, using Airborne Magnetic Data. *International Journal of Advanced Geosciences*, vol. 8 (2), pp. 263 - 271.
17. Egwuonwu, G. N., Ezech, O. C., Jegede, S. I., Umego, M. N. (2021) “Two-Dimensional Modeling of Subsurface Magnetic Lithology in Sokoto Basin, Northwestern Nigeria” Published in *International Research Journal of Innovations in Engineering and Technology - IRJIET*, Volume 5, Issue 1, pp 40-45. Article DOI <https://doi.org/10.47001/IRJIET/2021.501005>